Available online at www.sciencedirect.com
SCIENCE DIRECT®
Physics Letters A 335 (2005) 394–401
PHYSICS LETTERS A
www.elsevier.com/locate/pla

Finite-time Lyapunov spectrum for chaotic orbits of non-integrable Hamiltonian systems

J.D. Szezech Jr., S.R. Lopes *, R.L. Viana

Departamento de Física, Universidade Federal do Paraná, 81531-990 Curitiba, Paraná, Brazil

Received 3 August 2004; received in revised form 2 December 2004; accepted 3 December 2004

Available online 5 January 2005

Communicated by C.R. Doering

Abstract

We claim that dynamical traps displayed by chaotic orbits of non-integrable Hamiltonian systems can be characterized using properties of the finite-time Lyapunov exponent. We show that, for the case where the phase space presents stickiness regions, the distribution of the finite-time Lyapunov exponent is bimodal, while, for the case where no such regions exist, the distribution is a Gaussian-like one.

PACS: 05.45.Pq

1. Introduction

The phase space of non-integrable Hamiltonian systems is neither entirely regular, nor entirely chaotic. Both dynamical regimes are connected by a complicated layer where regular and irregular motion can or cannot mix, depending on the number of degrees of freedom of the system, as well as on properties of the limiting surface itself. The regular dynamics consists of quasiperiodic orbits lying on tori and periodic orbits, while chaotic orbits fill densely other parts of the energy surface [1]. In general, new features such as dynamical traps [2] and anomalous diffusion [3] appear in non-integrable dynamical systems as a result of the non-trivial combination of regularity and chaoticity, leading them to present unusual statistical properties for trajectories in the chaotic part of the phase space [4–7].

Dynamical traps in chaotic orbits are due to the stickiness of trajectories to some specific domains in phase space where a trajectory can spend an arbitrarily long (but) finite time. Such behavior for the trajectories can be due to hierarchical-islands trap, net-traps or stochastic layer traps [2]. In such phase space domains, parts of the trajectories are almost regular, in spite of the full trajectories being chaotic. There was shown, recently, that the topology for almost the whole

* Corresponding author.
E-mail address: lopes@fisica.ufpr.br (S.R. Lopes).

0375-9601/$ – see front matter
doi:10.1016/j.physleta.2004.12.058

phase space of smooth Hamiltonian systems presents fractal or multi-fractal properties, where regular and chaotic trajectories are arbitrarily close to each other [8,9]. Even when the phase space looks totally chaotic it is possible to find an infinite number of small (microscopic) islands wherein the trajectories are regular [10]. Important physical situations, for example, non-Gaussian (anomalous) transport in fluids or anomalous trajectories diffusion in general systems, can be related to the presence of regions of stickiness in the phase space [11]. Such topics can be useful in calculation of particle loss from plasmas and accelerators, rates of chemical reactions, wave heating rates in plasmas as well as in other areas of physics [12].

The presence of stickiness in some parts of the phase space of Hamiltonian systems—sometimes this aspect of the dynamics is called *pseudoergodicity* [13]—may yield some difficulties in the use of Lyapunov spectrum, since its computation supposes we have a good finite-time approximation for the ergodicity of the phase space. Such ergodic property may never hold completely, since Hamiltonian systems present regular islands embedded into the chaotic sea in phase space. Moreover, trajectories in the chaotic sea never enter any island, neither regular trajectories inside an island can reach the chaotic sea. In a first attempt, we can apply the ergodic property just for the chaotic part of the phase space. Nevertheless, even in this situation, the presence of trapping regions in the phase space can lead to arbitrarily large times for a trajectory to leave a particular part of the phase space. In this case the ergodic properties of the phase space may need a large amount of time to be verified. In a recent paper [14] dealing with a incompressible two-dimensional model for transport and mixing of flows (geophysical flows as exemplified in [14]), it was shown that the non-uniformity of the phase space and the presence of island of regular motion within the stochastic sea has considerable impact on the transport properties of some systems. For a extensive review of anomalous transport, fractional kinetics, pseudo-ergodicity and stickiness of trajectories see [15] and reference therein.

In this Letter we present how the dynamics of a non-integrable Hamiltonian system (exemplified by the standard map) can be understood using properties of the finite-time Lyapunov exponent (FTLE) [16]. The existence of Lyapunov exponents is proved under general conditions [17]. In a Hamiltonian non-hyperbolic system, chaotic and regular motions coexist in the phase space, which introduces large variations in local instability along a reference chaotic trajectory [18]. These variations are related to alternations between qualitatively different motions, such as chaotic and quasiregular (laminar) motions that can happen in low-dimensional systems [19], as well as in random and cluster motions in high-dimensional systems [20]. These variations are quantified by finite-time Lyapunov exponents, the exponential rates of principal divergences during finite-time intervals. Once trajectories trapping occurs just for a finite time, the use of FTLE is a way to quantify the trap effects. We show in this Letter that, using FTLE spectrum, dynamical traps can be numerically detected, and we can estimate how long the trajectories in the phase space are influenced by the trapping regions. By Leoncini and Zaslavsky [14] it was shown that small values of the FTLE distribution is correlated to the existence of long-lived jets in a two-dimensional model for fluid mixing and transport. In a dynamical point of view such jets is related to the stickiness of trajectories in some domain of the phase space and demonstrate some coherence for the flow model.

The Letter is organized as follows. In Section 2 we introduce the conservative dynamics of the standard map and present the definitions of numerical diagnostics to be used; Section 3 shows how the finite-time Lyapunov exponent can be used to quantify the total trapping time of chaotic orbits and, finally, in Section 4 we present our conclusions.

2. The dynamics of the standard map

The simplest Hamiltonian systems that can exhibit chaos are those having two degrees of freedom. The standard map is one of the most studied since it is a convenient model for studying chaotic behavior of Hamiltonian systems that yield a two-dimensional map. The standard map was introduced by Chirikov [21] as the discrete form of the equations for the kicked rotor characterized by the Hamiltonian

$$H(p,x,t) = \frac{1}{2}p^2 - K\cos x \sum_{n=-\infty}^{\infty} \delta(t-n), \qquad (1)$$

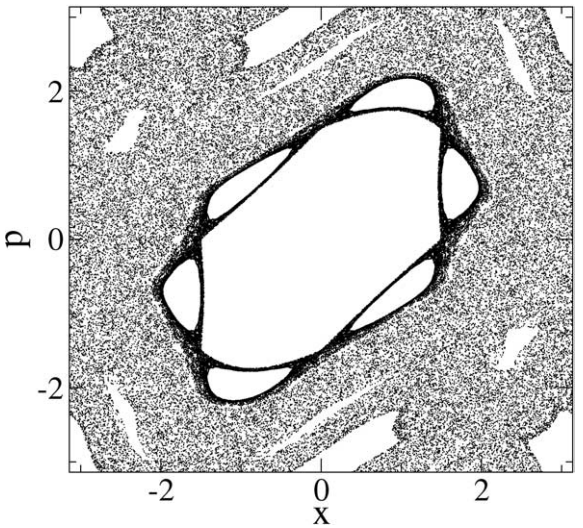

Fig. 1. Poincaré plot for the standard map for $K = 1.5$.

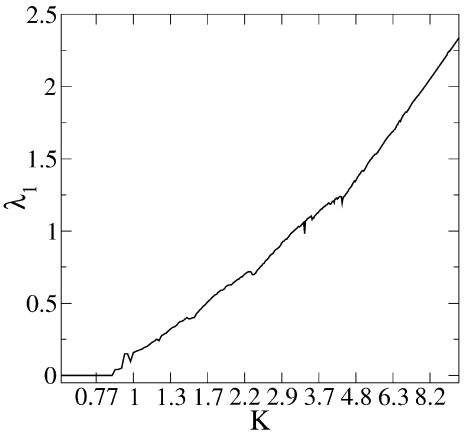

Fig. 2. Maximum Lyapunov exponent as a function of K for the standard map dynamics.

where p and x are the rotor angular momentum and positions, and K is the so-called non-linearity parameter. The map is considered on the torus, such that $p \in (-\pi, \pi)$ and $x \in (-\pi, \pi)$ and can be cast in the form:

$$p_{n+1} = p_n - K \sin x_n,$$
$$x_{n+1} = x_n + p_{n+1}, \tag{2}$$

where p_n and x_n are the rotor dynamical variable just after the nth kick given by the delta function in (1). Its is well known that, for $K > K_c \approx 0.9$ there is a large chaotic orbit, as evidenced by global stochastic scenario [1].

Firstly, we consider the case where the phase space has few domains of chaotic orbits. We start from a chaotic initial condition and iterate the map (2) until the resulting trajectories achieve good statistical properties. A Poincaré plot for the phase space in this case is depicted in Fig. 1.

For this particular value of K, the phase space is partially covered by quasiperiodic islands. The figure presents dark regions surrounding some islands as a result of the trapping suffered by the trajectories in their neighborhoods. In circumstances like this one, a superficial analysis of the Lyapunov spectrum can lead us to erroneously conclude about a regular motion for the system or even a smaller value for the positive Lyapunov exponent than the one actually presented by the dynamics [2]. The general effect of the trapping domains in the value of the Lyapunov exponent can be examined in Fig. 2, where the maximal Lyapunov exponent is shown as a function of the K parameter. Three different regimes can be observed: (i) for small values of K, the Lyapunov exponent value grows slowly, since for this interval $(0.8 < K < 2.2)$, the influence of the trap domains is more effective; (ii) above this regions in the parameter space the breakdown of some islands makes the trapping domains diminish and the Lyapunov exponent grows quicker between $2.2 < K < 4.7$; (iii) for values of $K > 4.7$ no more islands of appreciable size are noticed in phase portraits and the change of the Lyapunov exponent suddenly increases and present an almost constant slope as K grows.

Such situation can be better understood by the use of the FTLE. Since it measures local rates of the divergence or contraction of the phase space, it turns to be a more appropriate tool to evaluate the trapping influence in the total dynamics of the system. Let $(p, x)^{\mathrm{T}} \mapsto \mathcal{M}(p, x)^{\mathrm{T}}$ be the standard map (2), and n be a positive integer, such that $D\mathcal{M}^n(p_0, x_0)$ denotes the Jacobian matrix of the n-times iterated map, evaluated at the point (p_0, x_0). The eigenvalues of $D\mathcal{M}^n(p_0, x_0)$ are $\sigma_1(p_0, x_0, n) \geqslant \sigma_2(p_0, x_0, n)$.

We define the kth time-n Lyapunov exponent associated with the point (p_0, x_0) as

$$\lambda_k(p_0, x_0, n) = \frac{1}{n} \ln\left(\left\| D\mathcal{M}^n(p_0, x_0)\mathcal{U}_k \right\|\right) \quad (k = 1, 2), \tag{3}$$

where $\mathcal{U}_k$ is the eigenvector corresponding to the eigenvalue σ_k.

The FTLEs depend on the initial condition (p_0, x_0), whereas their infinite-time counterparts

$$\lambda_k = \lim_{n\to\infty} \lambda_k(p_0, x_0, n) \tag{4}$$

have the same value for almost every point (p_0, x_0).

The highly irregular behavior of the FTLE, alternating average contractions and repulsions, as a typical chaotic orbit wanders through its accessible phase space region, makes it useful to define a probability distribution. Let $f(\lambda_k(p_0, x_0, n))$ denote the probability density of the kth FTLE, when the initial condition (p_0, x_0) is chosen at random according to the Lebesgue measure of the chaotic orbit. In other words, $f(\lambda_k(n), n)\, d\lambda_k$ is the probability that the FTLE value lies between λ_k and $\lambda_k + d\lambda_k$.

If $\mathcal{F}(\lambda_k(n), n)$ is any function of the FTLE, its average over the invariant chaotic measure is given by

$$\overline{\mathcal{F}(\lambda_k(n))} = \frac{\int_{-\infty}^{+\infty} \mathcal{F}(\lambda_k(n))\, f(\lambda_k(n), n)\, d\lambda_k}{\int_{-\infty}^{+\infty} f(\lambda_k(n), n)\, d\lambda_k}. \tag{5}$$

To obtain the distribution $f(\lambda_k(n))$ numerically, we picked up many randomly chosen initial conditions uniformly distributed over the phase space region available to the chaotic orbit, and iterate each initial condition (p_0, x_0) a large number of times. Every $n = 100$ step we compute the time-100 exponent according to Eq. (3). Actually, we use the recurrence of chaotic orbits and follows a single chaotic trajectory a large number of steps. The FTLEs are then computed from conservative and non-overlapping length-100 sections of the trajectory. From these exponents we compute a frequency histogram, such depicted in Fig. 3. This figure shows the distribution for $\lambda_1(100)$ (dotted line) and $\lambda_2(100)$ (full line). Each distribution has two maxima (bimodal histogram) as we should expect.

Such distributions can be understood since, when the trajectory is in a trap near some island, the time-n Lyapunov exponent value corresponding to that piece is very small, and the FTLE distribution shows a small secondary maximum near zero. On the other hand, when the trajectory is in the bulk of the chaotic sea, the distribution presents values near the primary maximum. Since the system is area preserving, the second Lyapunov exponent distribution is symmetric to the first.

Fig. 4 presents the phase space of the system for a value of $K = 6.0$. In such case, just a few visible domains of the phase space are covered by islands. Hence, the trapping of the trajectories will happen just near these islands, and we expect that orbits will stay almost manly in the chaotic sea bulk. Fig. 5 presents the FTLE distribution for this situation (only the λ_1 exponent is shown, since the other distribution is symmetric with respect to $\lambda = 0$), and shows that the maximum near zero is much less observable.

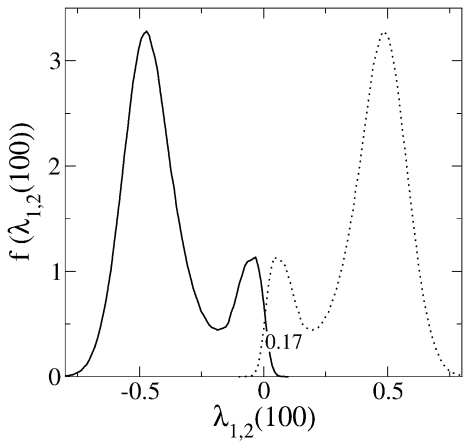

Fig. 3. Finite-time Lyapunov distribution for the standard map for $K = 1.5$.

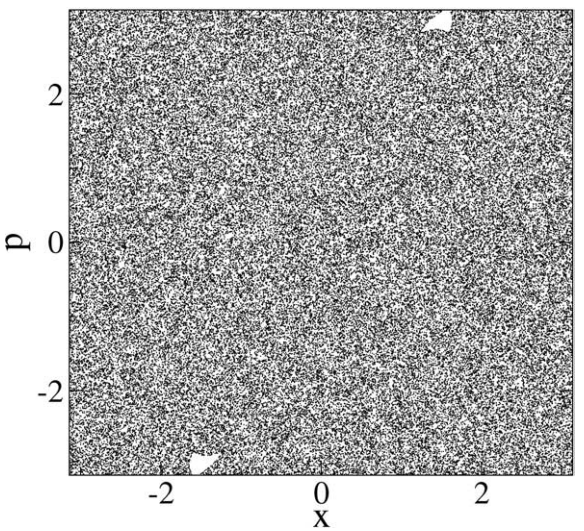

Fig. 4. Poincaré plot for the standard map for $K = 6.0$.

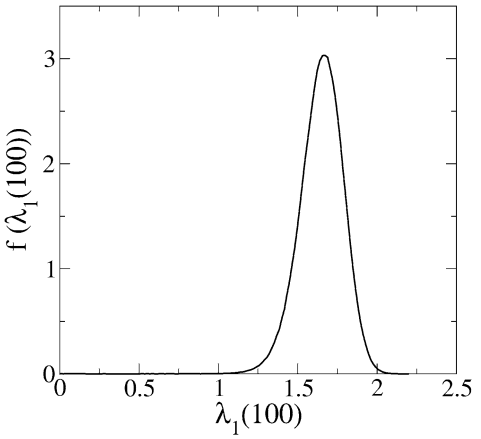

Fig. 5. Finite-time Lyapunov distribution for the standard map for $K = 6.0$.

For n large enough, the form of the distribution of the FTLE is [22]

$$f_G\big(\lambda_k(n), n\big) \approx \sqrt{\frac{nG''(\lambda_k)}{2\pi}}\exp\big[-nG(\lambda_k)\big], \tag{6}$$

where λ_k is the infinite-time limit of $\lambda_k(n)$, and the function $G(\lambda)$ has the following properties:

$$G(\lambda_k) = G'(\lambda_k) = 0, \qquad G''(\lambda_k) > 0. \tag{7}$$

Expanding $G(\lambda)$ in the vicinity of λ_k, the first non-vanishing term is the quadratic one, i.e., $f_G(\lambda_k)$ is expected to have a Gaussian shape (for $n \gg 1$)

$$f_G\big(\lambda_k(n), n\big) \approx \sqrt{\frac{nG''(\lambda_k)}{2\pi}} \times \exp\left[-\frac{nG''(\lambda_k)}{2}\big(\lambda_k(n) - \lambda_k\big)^2\right]. \tag{8}$$

This unimodal distribution has a unique maximum at $\lambda_k(n) = \lambda_k$, such that the average exponent is

$$\overline{\lambda_k(n)} = \lambda_k, \tag{9}$$

what also follows from direct integration of (8).

Gaussian distribution (8) actually follows from the central limit theorem. In presence of stickiness effects, this reasoning no longer applies and the distribution turns to be bimodal, with a primary maximum near (less than) $\overline{\lambda_k}$ as in the unimodal case and a secondary maximum near zero, due to the trapping caused by the proximity of quasiperiodic tori inside the resonant islands (trajectories strictly on those tori have zero Lyapunov exponent).

3. Total trapping time

The time fraction that the system stays under influence of a trap is an important diagnostic for the dynamics of the system. It can be inferred by computing the area under the secondary maximum of the Lyapunov distribution. This area is computed defining the relative minimum for the distribution $\lambda_{\min}$, calculated by the condition $df/d\lambda = 0$, and occurs between both maxima. We consider that the trajectory leaves the trap region when the finite value for the Lyapunov exponent is bigger than $\lambda_{\min}$. A particular value of this fraction is also plotted in Fig. 3 (17%) and gives us a glimpse on how important are the trap domains in the whole dynamics of the system.

As the non-linearity parameter K increases, the influence of the trapping turns to be smaller in general. This can be seen in Fig. 6(a), where we plot the fraction of time that the dynamics is under influence of a trap region as a function of the K parameter. A more detailed analysis of Fig. 6(b) and (c), where two magnifications of Fig. 6(a) are shown, suggest that the curve is not smooth, presenting many bursts. Hence, the influence of trapping domains is not a smooth function of the non-linear parameter K. It is possible to find a infinite number of island immersed into the chaotic sea as a result of resonances in the dynamics. A careful analysis of these bursts will show some degree of self-similarity. This behavior for the FTLE spectrum is compatible with the behavior presented by the phase space properties of Hamiltonian systems [2] and have the advantage to exhibit more clearly the effect of the trapping domains into the whole dynamics of the system.

Another property of some Hamiltonian system, namely, the fact that phase space can present the so-called cantorian torus [11,23,24] can also be observed by the use of FTLE. We plot in Fig. 7 the well know major KAM cantorus break up for the standard map, that occurs for $K \approx 0.971635406$ [11]. Fig. 7(a) presents the phase space before the crossing of the cantorus for a K value of 0.98 (lightly above the critical value), while Fig. 7(b) shows the same phase space,

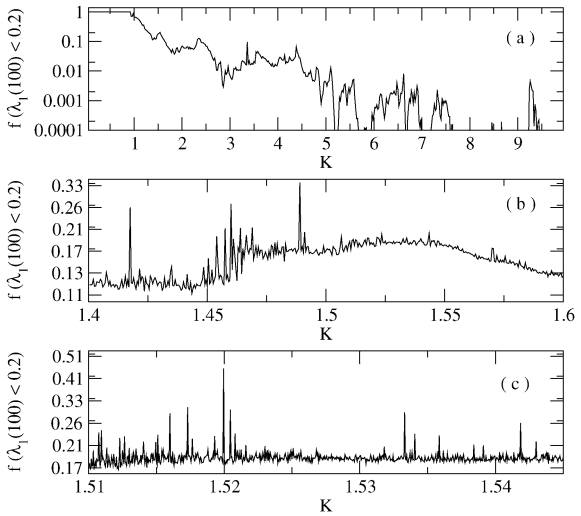

Fig. 6. Behavior of the finite-time Lyapunov exponent distribution as a function of the parameter K.

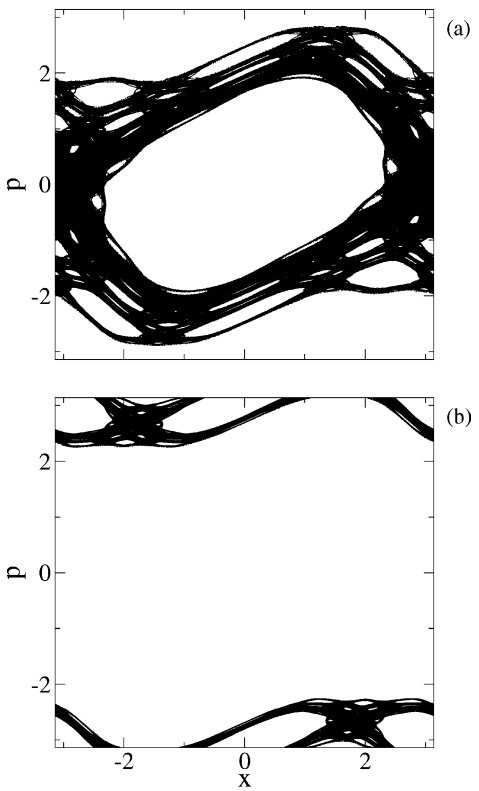

Fig. 7. Phase space for the standard map before (a) and after (b) the major cantorus crossing $K = 0.98$.

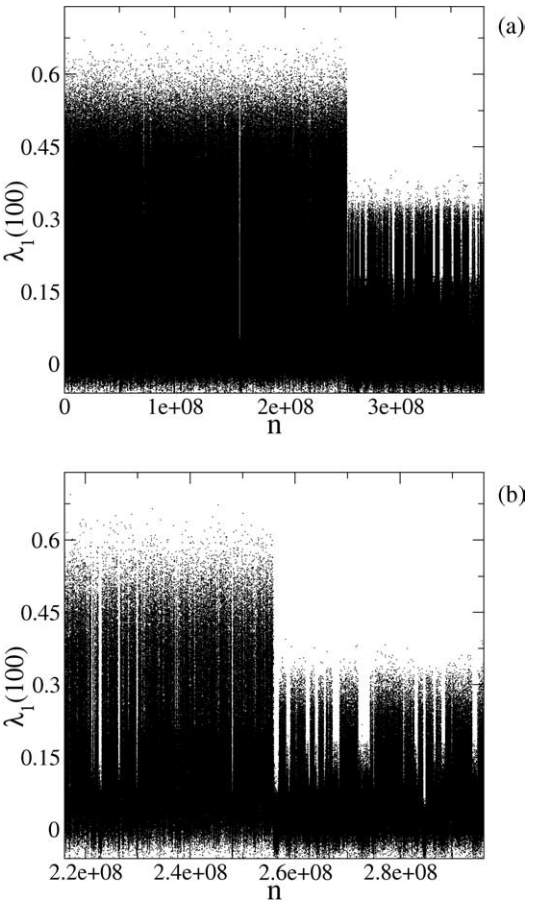

Fig. 8. (a) Signature of the cantorus crossing in the time series for the greatest FTLE. (b) Magnification of the crossing area. Maximums value of the FTLE below 0.2 are due to stickness effects, and exist before and after the cantorus crossing.

for the same K-value but, after the cantorus crossing. In order to show how the cantorus crossing signature is displayed in the FTLE time series, Fig. 8(a) presents the greatest FTLE time series. As can be observed the first cross of the cantorus occurs in $n \approx 2.5 \times 10^8$ in the figure. As a result of a more restrictive phase space after the cross of the cantorus, the time series presents maximums around 0.3 while before the crossing it was around 0.5.

An important question that arises when using FTLE is the fact that the result may be time-dependent. In other words, if the system would be observed for a longer time, the result could or could not be different. In order to clarify this point we plot in Fig. 9 the

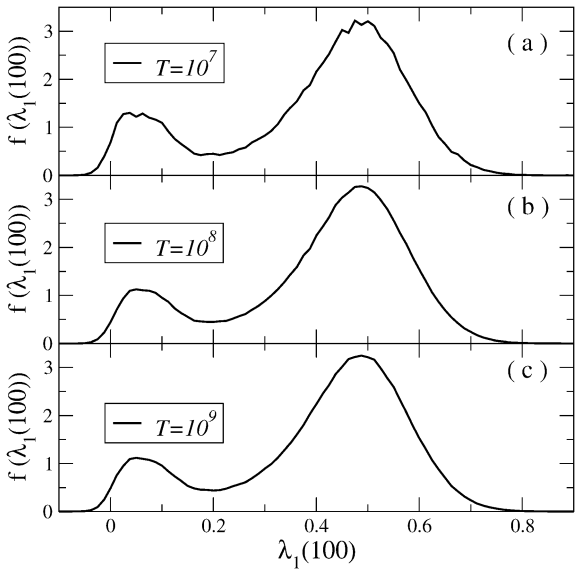

Fig. 9. Behavior of the finite-time Lyapunov exponent as a function of the time used to compute the exponent.

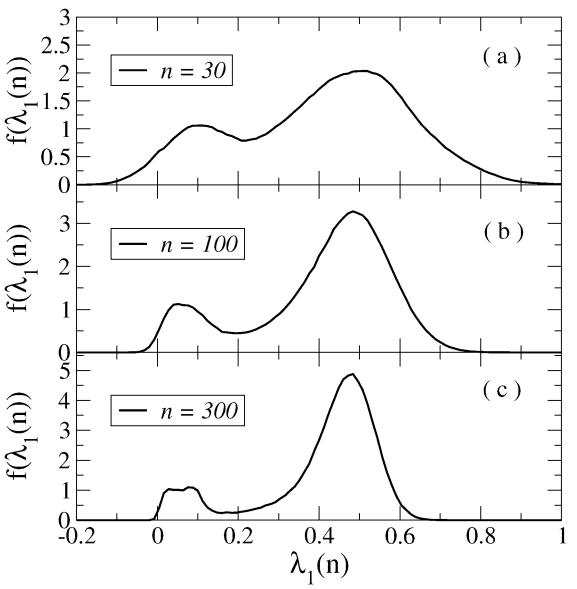

Fig. 10. Behavior of the finite-time Lyapunov exponent as a function of the time-stamp used to compute the exponent.

FTLE distribution for three trajectory lengths (T) for a $K = 1.5$ value. The results are not sensitive to the total time we iterate the system. Such result can be understood since for Hamiltonian systems, the longer are the trajectory times the higher the probability to enter in a trap. Moreover, the longer is the trajectory length the likely the system finds trap regions with longer trap times. Hence finite-time Lyapunov exponents can be used to measure how important are trap regions in the system dynamics, as long as we have a good statistical representation for the entire phase space.

As a final remark, we found that our results are not influenced by the time-stamp n of the FTLE. In Fig. 10 we plot the FTLE spectrum for $K = 1.5$, for three different time-stamps, and distributions do not change noticeably when the time-stamp of the exponent is changed from $n = 30$ to 300.

4. Conclusions

We have shown that the use of FTLE distributions can be useful to analyze the influence of trapping domains in the dynamics of Hamiltonian systems. While a bulk chaotic orbit typically shows a Gaussian-like distribution for the FTLE, centered at the infinite-time value; orbits suffering trapping effects develop a second maximum near zero. The use of FTLE distributions can also quantify the influence of the traps in the whole dynamics, given us the fraction of time the system stays under influence of the traps, by computing the relative area under the secondary maximum.

Our results are robust in the sense that they are rather insensitive to changes in the FTLE time-stamp n and the total trajectory length. Although we have used the standard map as a representative example of the stickiness phenomenon, we claim that our results are still valid for a wide class of non-integrable dynamical systems.

Acknowledgements

This work was partially supported by CNPq, CAPES and FINEP.

References

[1] A. Lichtenberg, A. Liberman, Regular and Chaotic Dynamics, Springer, Berlin, 1992.
[2] G.M. Zaslavsky, Physica D 168–169 (2002) 292.
[3] V. Latora, Phys. Rev. Lett. 83 (1999) 2104.
[4] C. Karney, Physica D 8 (1983) 360.

[5] J. Hanson, J. Cary, J. Meiss, J. Stat. Phys. 39 (1985) 327.
[6] J. Meiss, E. Ott, Physica D 20 (1986) 387.
[7] L. Kuznetsov, G.M. Zaslavsky, Phys. Rev. E 66 (2002) 046212.
[8] S. Denisov, J. Klafter, M. Urbakh, S. Flach, Physica D 170 (2002) 131.
[9] E. Ott, Chaos in Dynamical Systems, Cambridge Univ. Press, Cambridge, 1993.
[10] M.F. Shlesinger, G. Zaslavsky, J. Klafter, Nature 363 (1993) 31.
[11] R.S. Mackay, J.D. Meiss, I.C. Percival, Physica D 13 (1984) 55.
[12] A. Iomin, D. Gangardt, S. Fishman, Phys. Rev. E 57 (1998) 4054.
[13] G.M. Zaslavsky, Chaos 5 (1995) 653.
[14] X. Leoncini, G.M. Zaslavsky, Phys. Rev. E 65 (2002) 046216.
[15] G.M. Zaslavsky, Phys. Rep. 371 (2002) 461.
[16] S. Dawson, C. Grebogi, T. Sauer, J.A. Yorke, Phys. Rev. Lett. 73 (1994) 1927.
[17] S. Wiggins, Introduction to Applied Nonlinear Dynamical Systems and Chaos, Springer-Verlag, New York, 1990.
[18] T. Okushima, Phys. Rev. Lett. 91 (2003) 254101.
[19] M.A. Sepúlveda, R. Badii, E. Pollak, Phys. Rev. Lett. 63 (1989) 1226.
[20] T. Konishi, K. Kaneko, J. Phys. A 25 (1991) 6283.
[21] B.V. Chirikov, Phys. Rep. 52 (1979) 264.
[22] E.J. Kostelich, I. Kan, C. Grebogi, E. Ott, J.A. Yorke, Physica D 109 (1997) 81.
[23] I.C. Percival, in: M. Month, J.C. Herrera (Eds.), Nonlinear Dynamics and the Beam–Beam Interaction, in: American Institute of Physics Conference Proceedings, vol. 57, 1979, p. 302.
[24] S. Aubry, in: A.R. Bishop, T. Schneider (Eds.), Solitons and Condensed Matter Physics, Springer, Berlin, 1978, p. 264.